

Manuscript Number:

Title: Optimizing pre-eruptive temperature estimates in thermally and chemically zoned magma chambers

Article Type: Research Article

Keywords: clinopyroxene; thermometer; Sabatini Volcanic District; Campi Flegrei Volcanic Field

Corresponding Author: Dr. Silvio Mollo,

Corresponding Author's Institution: Istituto Nazionale di Geofisica e Vulcanologia

First Author: Silvio Mollo

Order of Authors: Silvio Mollo; Matteo Masotta

**Abstract:** We present a method to minimize the error of temperature estimate when multiple discrete populations of glass and clinopyroxene occur in a single heterogeneous eruptive unit. As test data we have used ~1100 clinopyroxene-melt pairs from isothermal and thermal gradient experiments. These latter are characterized by the crystallization of multiple modes of clinopyroxene as frequently documented for chemically and thermally zoned magma chambers. Equilibrium clinopyroxene-melt pairs are identified through the difference between predicted and measured components in clinopyroxene. The use of these equilibrium compositions as input data for the clinopyroxene-based thermometer demonstrates that the error of temperature estimate is minimized and approaches to the calibration error of the thermometric model. To emphasize the paramount importance of this approach for predicting the crystallization temperature of heterogeneous magmas, we have tested our method by means of ~480 and ~150 clinopyroxene-melt pairs from the explosive eruptions of the Sabatini Volcanic District (Latium Region, Central Italy) and the Campi Flegrei Volcanic Field (Campanian Region, Southern Italy), respectively. These eruptions were fed by zoned magma chambers, as indicated by the occurrence of multiple modes of clinopyroxene in the eruptive units. Results from calculations demonstrate that clinopyroxene-melt pairs in equilibrium at the time of eruption are effectively captured by our method; consequently, the error of temperature estimate due to the accidental use of disequilibrium compositions is significantly reduced.

1 **Optimizing pre-eruptive temperature estimates in thermally and chemically**  
2 **zoned magma chambers**

3 Silvio Mollo<sup>1</sup> and Matteo Masotta<sup>2</sup>

4 <sup>1</sup> Istituto Nazionale di Geofisica e Vulcanologia, Via di Vigna Murata 605, 00143 Roma, Italy

5 <sup>2</sup> Bayerisches Geoinstitut, Universität Bayreuth, Bayreuth, Germany

6

7 Corresponding author:

8 Dr. Silvio Mollo

9 Istituto Nazionale di Geofisica e Vulcanologia

10 Via di Vigna Murata 605

11 00143 Roma - ITALY

12 office tel. +39 0651860674

13 lab tel. +39 0651860223

14 fax +39 0651860507

15

16

17

18

19

20

21

22

23

24

25

26 **ABSTRACT**

27 We present a method to minimize the error of temperature estimate when multiple discrete  
28 populations of glass and clinopyroxene occur in a single heterogeneous eruptive unit. As test  
29 data we have used ~1100 clinopyroxene-melt pairs from isothermal and thermal gradient  
30 experiments. These latter are characterized by the crystallization of multiple modes of  
31 clinopyroxene as frequently documented for chemically and thermally zoned magma  
32 chambers. Equilibrium clinopyroxene-melt pairs are identified through the difference between  
33 predicted and measured components in clinopyroxene. The use of these equilibrium  
34 compositions as input data for the clinopyroxene-based thermometer demonstrates that the  
35 error of temperature estimate is minimized and approaches to the calibration error of the  
36 thermometric model. To emphasize the paramount importance of this approach for predicting  
37 the crystallization temperature of heterogeneous magmas, we have tested our method by  
38 means of ~480 and ~150 clinopyroxene-melt pairs from the explosive eruptions of the  
39 Sabatini Volcanic District (Latium Region, Central Italy) and the Campi Flegrei Volcanic  
40 Field (Campanian Region, Southern Italy), respectively. These eruptions were fed by zoned  
41 magma chambers, as indicated by the occurrence of multiple modes of clinopyroxene in the  
42 eruptive units. Results from calculations demonstrate that clinopyroxene-melt pairs in  
43 equilibrium at the time of eruption are effectively captured by our method; consequently, the  
44 error of temperature estimate due to the accidental use of disequilibrium compositions is  
45 significantly reduced.

46

47

48 **Keywords:** clinopyroxene; thermometer; Sabatini Volcanic District; Campi Flegrei Volcanic  
49 Field

50

## 51 1.1 INTRODUCTION

52 Despite Clinopyroxene composition is frequently used to retrieve the crystallization  
53 temperature of magmas, the systematic error of temperature estimate resulting from the  
54 accidental use of disequilibrium clinopyroxene-melt pairs is one important limitation of  
55 clinopyroxene-based thermometers (Putirka 2008; Mollo et al., 2010). This aspect is  
56 emphasized in thermally and compositionally zoned magma chambers that feed explosive  
57 eruptions worldwide. Recharge by magmas carrying crystals equilibrated at different depths  
58 as well as crystal sinking in long-lived magma chambers may cause the coexistence of  
59 equilibrium and disequilibrium clinopyroxenes in the eruptive products (Fridrich and  
60 Mahood, 1987; Boden, 1989; Schuraytz, 1989; Streck and Grunder, 1997; Evans and  
61 Bachmann, 2012). Multiple discrete populations of clinopyroxene (and less frequently glass)  
62 have been documented at single stratigraphic horizons of voluminous heterogeneous eruptions  
63 associated to zoned magma chambers (e.g., Matthews et al., 1999). The use of these  
64 compositionally different phases as input data for thermometers leads to a considerable scatter  
65 of the temperature estimate with high- and low-temperature outliers (e.g., Cathey and Nash,  
66 2004).

67 Stratified magma chambers are generally produced by (i) repeated influxes of hydrous  
68 mafic magmas from the mid to lower crust into the shallow silicic zone (Matthews et al.,  
69 1999; Bachmann et al., 2012), (ii) the supply of heat from a mantle source to the base of an  
70 evolving crustal magma reservoir tapped by multiple eruptions (Cathey and Nash, 2003), and  
71 (iii) abundant fractionation and accumulation of crystals through time forming a stratified  
72 mush zone (D'Antonio, 2011; Deering et al., 2011; Masotta et al., 2012). In the light of these  
73 frequent disruption processes, the key question is: when multiple discrete populations of  
74 clinopyroxene and glass occur in the same erupted product, how can we recognize  
75 clinopyroxene-melt pairs in equilibrium at the time of eruption, in order to minimize the error

76 of temperature estimate? Recently, [Mollo et al. \(2013\)](#) presented new global regression  
77 analyses that improved those by [Putirka \(1999\)](#) in testing the equilibrium between  
78 clinopyroxene and coexisting melt. To date, this model has been tested through  
79 clinopyroxene-melt pairs obtained from controlled cooling rate experiments simulating the  
80 solidification of a few-metre-thick dike or lava ([Mollo et al., 2010](#)). But it is clear that, these  
81 post-eruptive conditions are not applicable to the case of thermally zoned magma chambers.  
82 Therefore, there is no guarantee that the activity model of [Mollo et al. \(2013\)](#) can be used to  
83 minimize the error of temperature estimate when multiple discrete populations of  
84 clinopyroxene are found in eruptive products associated to large, long-lived magma  
85 chambers.

86 To remedy this deficiency, we present new tests conducted on heterogeneous populations  
87 of clinopyroxene and glass from thermal gradient experiments and heterogeneous volcanic  
88 units. Thermal experiments were designed to reproduce the disruption processes of  
89 crystallization, differentiation and crystal-melt separation that are observed in chemically and  
90 thermally zoned magma chambers ([Blake, 1981](#); [Blake and Ivey, 1986](#); [Matthews et al., 1999](#);  
91 [Wallace et al., 1999](#); [Cathey and Nash, 2004](#); [Wark et al., 2007](#); [Masotta et al., 2012](#)). Our  
92 results demonstrate that the occurrence of multiple clinopyroxene-melt pairs cause a  
93 systematic error of temperature estimate, whose magnitude can be now quantified. To  
94 emphasize the paramount importance of this approach for estimating pre-eruptive  
95 temperatures, we have applied our method to two distinct explosive heterogeneous eruptions  
96 occurred in Italy and fed by zoned magma chambers. Using natural clinopyroxene and melt  
97 compositions from these eruptions, we prove that the method presented in this study  
98 effectively captures clinopyroxene-melt pairs in equilibrium at the time of crystallization, thus  
99 significantly reducing the error of temperature estimate.

100

## 101 2.1 OVERVIEW OF THE METHOD

102 In an early study, [Putirka \(1999\)](#) observed that the degree of disequilibrium for  
103 clinopyroxene-bearing rocks may be determined through the comparison between  
104 clinopyroxene components predicted by empirical equations obtained via regression analyses  
105 of clinopyroxene-melt pairs from isothermal experiments, and those measured in natural  
106 products. Following this approach, [Mollo et al. \(2013\)](#) proposed an improved predictive  
107 equation for equilibrium that were calibrated on global regression analyses of ~1200  
108 clinopyroxene-melt pairs from literature:

109

$$\ln(X_{DiHd}^{cpx}) = -2.18 - 3.16X_{TiO_2}^{melt} - 0.365\ln(X_{AlO_{1.5}}^{melt}) + 0.05\ln(X_{MgO}^{melt})$$
$$- 3858.2 \frac{(X_{EnFs}^{cpx})^2}{T(K)} + \frac{2107.4}{T(K)} - 17.64 \frac{P(kbar)}{T(K)}$$

110

111

$$112 \quad (R^2 = 0.92; \text{SEE} = 0.06) \quad (1)$$

113

114 The equilibrium equation (1) is highly correlated with the deviation between observed and  
115 calculated values of DiHd (diopside + hedenbergite) and EnFs (enstatite + ferrosilite). From a  
116 theoretical point of view, this means that the error of temperature estimate (ETE)  
117 progressively decreases as the difference ( $\Delta$ ) between predicted and measured components in  
118 clinopyroxene goes to zero. The aim of this study is to demonstrate that the activity model (1)  
119 can be used to minimize the error of temperature estimate when multiple discrete populations  
120 of glass and clinopyroxene coexist in a single eruptive unit. To do this, we have used as input  
121 data ~1100 clinopyroxene-melt pairs from isothermal and thermal gradient experiments  
122 conducted by [Masotta et al. \(2012\)](#). Isothermal piston cylinder experiments were carried out  
123 at 300 MPa for 24 h. Clinopyroxenes were equilibrated with tephriphonolite and phonolite  
124 melts at 1000, 950, 900 and 850 °C, over an oxygen fugacity defined by the NNO+2 buffer

125 and a melt-water content of 4 wt.%. The same conditions were used for two thermal gradient  
 126 experiments based on the innate temperature gradient of the piston cylinder assembly that  
 127 imposed an increasing temperature from the top (850 °C) to the bottom (1000 °C) of the  
 128 capsule (Fig. 1a; see Masotta et al., 2012 for further details). By means of textural and  
 129 compositional analyses as well as crystal settling models, Masotta et al. (2012) have  
 130 demonstrated that crystals and melts are chemically heterogeneous along the capsule due to  
 131 (i) the rapid extraction of the interstitial differentiated melt in the uppermost zone of the  
 132 capsule driven by compaction of the crystal mush (Fig. 1a), (ii) a considerable crystal sinking  
 133 testified by the U-shaped boundary between the glassy and the crystallized regions at the  
 134 bottom of the capsule (Fig. 1a), and (iii) the insufficient diffusion of major elements to ensure  
 135 melt homogenization over the experimental duration (Fig. 1b). These disruption processes led  
 136 to the formation of multiple discrete modes of clinopyroxene and glass (Fig. 1c) that resemble  
 137 those found in natural explosive eruptions fed by thermally zoned magma chambers (cf.  
 138 Masotta et al., 2010; 2012).

139 Equilibrium and disequilibrium clinopyroxene-melt pairs have been resolved by the  
 140 activity model (1) and their crystallization temperatures have been estimated by using the new  
 141 thermometric equation of Masotta et al. (2013) specific for alkaline differentiated magmas:

$$\begin{aligned}
 142 \quad & \\
 143 \quad & \frac{10^4}{T(\text{K})} = 2.91 - 0.40 \ln \left( \frac{X_{Jd}^{cpx} X_{Ca}^{liq} X_{Fm}^{liq}}{X_{DiHd}^{cpx} X_{Na}^{liq} X_{Al}^{liq}} \right) + 0.038(H_2O) - 1.64 \left( \frac{X_{Mg}^{liq}}{X_{Mg}^{liq} + X_{Fe}^{liq}} \right) + \\
 & + 1.01 \frac{X_{Na}^{liq}}{X_{Na}^{liq} + X_K^{liq}} - 0.22 \ln(X_{Ti}^{liq}) + 0.47 \ln \left( \frac{X_{Jd}^{cpx}}{X_{Na}^{liq} X_{Al}^{liq} (X_{Si}^{liq})^2} \right) + 1.62(K_{D(Fe-Mg)}^{cpx-liq}) + 23.39(X_{Ca}^{liq} X_{Si}^{liq}) \\
 144 \quad & \\
 145 \quad & (R^2 = 0.93; \text{SEE} = 18) \qquad \qquad \qquad (2) \\
 146 \quad &
 \end{aligned}$$

147 The equation (2) was obtained through new regression analyses based on previous activity  
148 models by [Putirka \(2008\)](#) and conducted on a calibration dataset restricted to trachyte, tephri-  
149 phonolite and phonolite magmas. On one hand, this strategy has improved the precision of the  
150 equation (2) as the standard error of estimate is very low ( $SEE = 18 \text{ }^\circ\text{C}$ ). On the other hand,  
151 the use of the global equations of [Putirka \(2008\)](#) rather than equation (2) is recommended  
152 when estimating the crystallization conditions of poorly differentiated magmas and other  
153 magma compositions not sufficiently represented into the calibration dataset.

154 Chemical analyses were carried out at the HP-HT Laboratory of Experimental  
155 Volcanology and Geophysics of Istituto Nazionale di Geofisica e Vulcanologia (Rome, Italy)  
156 with an Electronic Probe Micro Analysis (EPMA) Jeol-JXA8200 combined EDS-WDS (five  
157 spectrometers with twelve crystals). For glasses, a slightly defocused electronic beam with a  
158 size of  $3 \text{ }\mu\text{m}$  was used with a counting time of 5 s on background and 15 s on peak. For  
159 crystals, the beam size was  $1 \text{ }\mu\text{m}$  with a counting time of 20 and 10 s on peaks and  
160 background, respectively. The following standards have been adopted for the various  
161 chemical elements: jadeite (Si and Na), corundum (Al), forsterite (Mg), andradite (Fe), rutile  
162 (Ti), orthoclase (K), barite (Ba), apatite (P), spessartine (Mn) and chromite (Cr). Sodium and  
163 potassium were analyzed first to reduce possible volatilization effects. Precision was better  
164 than 5 % for all cations. All chemical data are reported in a [Microsoft Excel spreadsheet](#)  
165 available as supplementary material which also includes (i) the procedure for the calculation  
166 of clinopyroxene components ([Putirka et al., 1996](#); [Putirka, 2003, 2008](#)), (ii) the equilibrium  
167 equation of [Mollo et al. \(2013\)](#), and (iii) the thermometric model of [Masotta et al. \(2013\)](#).

168

## 169 **3.1 RESULTS AND DISCUSSION**

### 170 **3.1.1 A method to minimize the error of temperature estimate**



171 To test whether equation (1) may effectively capture equilibrium clinopyroxene-melt  
 172 pairs, we have used as input data compositions from isothermal and thermal gradient  
 173 experiments by Masotta et al. (2012). Results are plotted in Fig. 2a where the value of DiHd  
 174 predicted by equation (1) is compared with that measured for each clinopyroxene. The  
 175 compositions obtained at isothermal conditions plot within 2 % ( $\Delta\text{DiHd} \leq 0.02$ ) of the one-to-  
 176 one line suggestive of near-equilibrium crystallization (Fig. 2a). Conversely, thermal gradient  
 177 experiments show two distinct populations of clinopyroxene-melt pairs. The first population  
 178 consists of 195 clinopyroxene-melt pairs and exhibits  $\Delta\text{DiHd}$  values comparable to the near-  
 179 equilibrium compositions obtained from isothermal experiments. The second population  
 180 comprises the majority of the data (853 clinopyroxene-melt pairs) and significantly deviate  
 181 from the equilibrium straight line of the diagram ( $0.03 \leq \Delta\text{DiHd} \leq 0.20$ ). It is worth stressing  
 182 that near-equilibrium data show a positive correlation between the magnesium number [ $\text{Mg\#}$   
 183 =  $\text{MgO}/(\text{MgO}+\text{FeO}_{\text{tot}}) \times 100$  in mole fractions] of clinopyroxene and that of the melt (Fig. 2b):

$${}^{\text{melt}}\text{Mg\#} = 1.05^{\text{cpx}}\text{Mg\#} - 28.28$$

$$(\text{R}^2 = 0.95; \text{SEE} = 2) \quad (3)$$

188  
 189 The high coefficient of determination ( $\text{R}^2$ ) and the low SEE of equation (3) suggest the  
 190 achievement of equilibrium between clinopyroxene and melt as revealed by the model of  
 191 Mollo et al. (2013) (Fig. 2b). This outcome is also corroborated by MELTS (Ghiorso and  
 192 Sack, 1995) simulations performed at the same conditions adopted for isothermal  
 193 experiments. The regression analysis of clinopyroxene and melt compositions from MELTS  
 194 demonstrates that, in terms of equilibrium thermodynamics, there is a linear dependence  
 195 between  ${}^{\text{melt}}\text{Mg\#}$  and  ${}^{\text{cpx}}\text{Mg\#}$ . Moreover, the fitting parameters derived through MELTS

196 compositions are comparable to those of equation (3) obtained through the analyses of  
197 experimental data:

198

$$199 \quad {}^{melt}Mg\# = 1.11 {}^{cpx}Mg\# - 32.96$$

200

$$201 \quad (R^2 = 0.99; \text{SEE} = 0.6) \quad (4)$$

202

203 In this study, we also highlight that the activity model (1) is a more robust test for  
204 equilibrium than the Fe–Mg exchange reaction between clinopyroxene and melt. The study of  
205 [Putirka \(2008\)](#) has indeed improved this latter model showing a temperature dependence for  
206  ${}^{cpx-melt}Kd_{Fe-Mg}$  [ ${}^{cpx-melt}Kd_{Fe-Mg} = ({}^{cpx}Fe/{}^{melt}Fe) \times ({}^{melt}Mg/{}^{cpx}Mg)$ ]. However, at the same time  
207 the author pointed out that  ${}^{cpx-melt}Kd_{Fe-Mg}$  is not a reliable indicator of clinopyroxene–melt  
208 equilibrium for a wide range of compositions. This may occur if (i) the content of Fe is  
209 assumed as total iron (e.g., [Putirka et al., 2008](#); [Mollo et al., 2012](#)) and (ii) the content  $Fe^{2+}$  in  
210 clinopyroxene is derived by charge balance equations based on microprobe data ([Mollo et al.,](#)  
211 [2010, 2011](#)) rather than through more appropriate Mossbauer spectroscopic analyses  
212 ([McGuire et al., 1989](#)). We have used the improved model of [Putirka \(2008\)](#) to calculate the  
213 Fe–Mg exchange between clinopyroxene and melt from isothermal and thermal gradient  
214 experiments. All values for  ${}^{cpx-melt}Kd_{Fe-Mg}$  fall within the equilibrium range of  $0.27 \pm 0.03$   
215 reported by previous studies ([Grove and Bryan, 1983](#); [Sisson and Grove, 1993](#); [Putirka et al.,](#)  
216 [2003](#)); however, the equation (1) clearly indicates that a broad number of compositions  
217 deviate from the equilibrium condition ([Fig. 3a](#)).

218 To determine the magnitude of ETE caused by the accidental use of disequilibrium  
219 clinopyroxene–melt pairs, we have used the thermometric equation of [Masotta et al. \(2013\)](#)  
220 specific for alkaline differentiated magmas. Considering that  ${}^{melt}Mg\#$  is one of the most

221 important calibration parameters of thermometers (Putirka et al., 1996, 2003; Putirka, 1999,  
222 2008; Masotta et al., 2013), each predicted temperature has been compared with its value.  
223 Results are plotted in Fig. 3b showing that equilibrium compositions captured by equation (1)  
224 are linearly correlated with the temperatures predicted by the thermometer:

225

$$226 \quad {}^{melt}Mg\# = 0.19T(^{\circ}C) - 150.18$$

227

$$228 \quad (R^2 = 0.96; SEE = 2) \qquad (5)$$

229

230 The good fit of equation (5) underlines that near-equilibrium data ( $\Delta DiHd \leq 0.02$ ) yield an  
231 error of temperature estimate (ETE = 20 °C) very close to the standard error of estimate (SEE  
232 = 18 °C) obtained through the calibration of the thermometer. Rationally, each temperature  
233 prediction close to the regression line of Fig. 2a is affected by a low uncertainty whose value  
234 depends on (i) the best regression model derived for the thermometer and (ii) the 1 sigma  
235 error calculated from variations in replicated microprobe analyses. In contrast, any deviation  
236 from equilibrium causes that ETE becomes higher than SEE. In this respect, Fig. 3b shows  
237 that data with  $\Delta DiHd = 20$  yield a maximum value of the error of temperature estimate  
238 (ETE<sub>max</sub> = 85 °C) that is ~5 times higher than the SEE measured for the thermometer.

239

### 240 **3.1.2 Application to the Sabatini Volcanic District**

241 The Sabatini Volcanic District (Latium Region, Central Italy) produced voluminous  
242 explosive eruptions characterized by a wide spectrum of potassic rock-types with trachytic,  
243 tephriphonolitic and phonolitic compositions (Conticelli et al., 1997). The Tufo Giallo della  
244 Via Tiberina (TGVT) eruptive sequence groups a series of widespread pyroclastic deposits  
245 with estimated volume of about 10 km<sup>3</sup>. TGVT emplaced in the eastern sector of the volcanic

246 district through at least two main eruptive events at  $561\pm 1$  ka and  $550\pm 5$  ka, respectively  
247 (Karner et al., 2001). One of the most important features of TGVT is the coexistence of  
248 subaphyric-vitrophyric white pumice and highly crystalline black-grey scoria in the juvenile  
249 component. Using new petro-chemical data and MELTS modelling, Masotta et al. (2010)  
250 provided that these compositionally different juvenile clasts are due to the evolution of a  
251 shallow-level ( $\sim 150$  MPa), thermally zoned magma chamber. As documented for other  
252 voluminous eruptions in the world, the occurrence of multiple glasses and crystals in TGVT  
253 attests the tapping of thermally different regions (i.e., crystal-poor and crystal-rich regions) of  
254 the magma chamber in the course of individual explosive events (e.g., Blake, 1981; Matthews  
255 et al., 1999; Wallace et al., 1999; Cathey and Nash, 2003; Fowler and Spera 2010; Bachmann  
256 et al., 2012). This evolutionary process has been also corroborated by equilibrium and thermal  
257 gradient experiments of Masotta et al. (2012) reproducing the liquid line of descent of magma  
258 as well as the complex chemical (the compositional variation of phases) and textural (the  
259 different crystal content) features of the zoned magma chamber.

260 According to the above discussion, we have analyzed 483 clinopyroxene-melt pairs from  
261 the juvenile clasts of TGVT. All these data are reported in the Microsoft Excel spreadsheet  
262 available as supplementary material. On one hand, results from equation (1) indicate that the  
263 equilibrium crystallization was not the rule for TGVT (Fig. 4a); indeed, only 27  
264 clinopyroxene-melt pairs plot on the one-to-one line. On the second hand, isothermal  
265 experiments by Masotta et al. (2012) were conducted at crystallization conditions comparable  
266 to those of the Sabatini Volcanic District as well as to other active volcanic regions  
267 characterized by alkaline differentiated magmas (see the case study below). The experimental  
268 clinopyroxene-melt pairs suggest that near-equilibrium crystallization occurs for the  
269 compositions that plot within 2 % of the one-to-one line (Fig. 2a). In this respect, we extended  
270 the equilibrium dataset to 98 clinopyroxene-melt pairs showing  $\Delta \text{DiHd} \leq 0.02$  (Fig. 4a).

271 Obviously, to minimize the error of temperature estimate, the value of  $\Delta\text{DiHd}$  should be as  
272 lower as possible. However, this value would also change as a function of the composition of  
273 the magma, the crystallization conditions (e.g., pressure, temperature,  $\text{H}_2\text{O}$ , etc.) and the  
274 accuracy of microprobe analysis. For example, [Jeffery et al. \(2013\)](#) observed that the majority  
275 of natural clinopyroxene-melt pairs showing  $\Delta\text{DiHd} \leq 0.1$  were suitable for thermometric  
276 calculations conducted on basaltic-andesites and magmatic xenoliths from the Kelut volcano  
277 (East Java). As displayed in the  $^{\text{cpx}}\text{Mg\#}$  vs.  $^{\text{melt}}\text{Mg\#}$  diagram of [Fig. 4a](#), the equilibrium  
278 compositions are well reproduced by the following linear fit:

279

$$280 \quad {}^{\text{melt}}\text{Mg\#} = 0.98 {}^{\text{cpx}}\text{Mg\#} - 22.63$$

281

$$282 \quad (R^2 = 0.94; \text{SEE} = 3) \quad (6)$$

283

284 Since the slope and intercept of equation (6) are comparable to those of equations (3) and (4)  
285 obtained from experimental and MELTS data, we infer that the activity model (1) effectively  
286 captured the majority of equilibrium clinopyroxene-melt pairs formed at the time of TGVT  
287 eruption.

288 The thermometric equation of [Masotta et al. \(2013\)](#) has been used to estimate the  
289 crystallization temperature of TGVT magma. The melt-water content (5-6 wt.%) was  
290 determined by the “difference from 100” method based on the difference to 100 % of the total  
291 obtained by glass microprobe analysis ([Devine et al., 1995](#)). The thermometric model  
292 predicted a wide spectrum of pre-eruptive temperatures ranging from 860 to 1000 °C ([Fig.](#)  
293 [4b](#)). Despite the broad temperature distribution, the equilibrium clinopyroxene-melt pairs  
294 resolved by the equation (1) yield a crystallization temperature of  $890 \pm 25$  °C ([Fig. 4b](#)). This  
295 value agrees with the pre-eruptive temperatures deduced by [Masotta et al. \(2010\)](#) through

296 phase relationships from petrographic observations of juvenile clasts, and simulations based  
297 on thermodynamic models. Importantly, with respect to the temperature estimate of  $890\pm 25$   
298 °C, [Fig. 4b](#) highlights that the compositional heterogeneity of clinopyroxenes and glasses in  
299 TGVT causes great uncertainties. Indeed, when the error of temperature estimate is maximum  
300 ( $ETE_{\max} = 100$  °C), the temperature predicted by the thermometer may even oversteps the  
301 liquidus temperature (1000 °C) of the phonolitic parental magma (see [Masotta et al., 2010](#)).

302

### 303 **3.1.3 Application to the Campi Flegrei Volcanic Field**

304 The Campi Flegrei Volcanic Field (Campanian Region, Southern Italy) is an active  
305 volcanic region that covers an area of about 230 km<sup>2</sup>. It experienced two cataclysmic caldera-  
306 forming eruptions which produced the Campanian Ignimbrite (39 ka) and the Neapolitan  
307 Yellow Tuff (15 ka). The eruption of the Campanian Ignimbrite, an unwelded to partially  
308 welded trachytic-phonolitic ignimbrite, is regarded as the dominant event in the history of the  
309 Campi Flegrei Volcanic Field with a minimum bulk volume of about 310 km<sup>3</sup> and initial  
310 areal distribution of about 30000 km<sup>2</sup> ([Rolandi et al., 2003](#)). The plumbing system of the  
311 Campi Flegrei Volcanic Field is still under debate and two main hypothesis have been  
312 evoked: (i) the presence of different magma batches evolved in separated magma chambers  
313 ([Pabst et al., 2007](#)) and (ii) the evolution of a unique shallower magmatic reservoir  
314 ([Pappalardo and Mastrolorenzo, 2012](#)). However, several geochemical, petrological and  
315 geophysical data are in favor of this second hypothesis. In fact, isotopic investigations have  
316 pointed out that magmas evolve in a compositionally zoned magma chamber ([Pappalardo et](#)  
317 [al., 2002](#)). Thermo-dynamical modeling and phase-equilibrium experiments have also  
318 demonstrated that shallower (250–150 MPa) crystal-poor felsic magmas with ~3 wt.% H<sub>2</sub>O  
319 are supplied by a deeper crystal-rich mafic layer ([Signorelli et al. 1999](#); [Fowler et al. 2007](#);  
320 [Fabrizio and Carroll, 2008](#); [Pappalardo et al., 2008](#)). The presence of a unique shallow

321 magmatic source is also supported by geophysical data underling the existence of a partial  
322 melting zone at 7–8 km depth where trachyphonolitic magmas originates by differentiation of  
323 a voluminous parent shoshonitic liquid (D'Antonio, 2011). This evolutionary process would  
324 lead to the formation of crystal mushes dominated by mafic phases (clinopyroxene and  
325 olivine) and significant amounts of melt directly correlated to the seismic wave velocity  
326 anomaly measured widespread beneath the caldera (Zollo et al., 2008). Therefore, the  
327 plumbing system of the Campi Flegrei Volcanic Field appears to be comparable to other  
328 zoned chambers that fed voluminous explosive eruptions in the world (e.g., Blake, 1981;  
329 Blake and Ivey, 1986; Wallace et al., 1999; Wark et al., 2007).

330 In this study, we have collected the chemical analyses of clinopyroxene and glass reported  
331 for the Campanian Ignimbrite by several authors (Melluso et al., 1995; Civetta et al., 1997;  
332 Signorelli et al., 1999; Pappalardo et al., 2002, 2008; Webster et al., 2003; Fulignati et al.,  
333 2004; Marianelli et al., 2006; Fedele et al., 2008, 2009). The dataset consists of 148  
334 clinopyroxene-melt pairs and is reported in the [Microsoft Excel spreadsheet](#) available as  
335 supplementary material. The Campanian Ignimbrite eruption contains a broad range of  
336 clinopyroxene and glass compositions testifying to the heterogeneity of the magmatic system  
337 (Fig. 5a). Using clinopyroxene-melt pairs as input data for the equation (1), we observe that  
338 only 60 clinopyroxene melt-pairs indicate equilibrium or near equilibrium crystallization  
339 ( $\Delta\text{DiHd} \leq 0.02$ ) at the time of eruption (Fig. 5b). This seems to corroborate the hypothesis of  
340 a thermally and chemically zoned magma chamber feeding the Campanian Ignimbrite  
341 eruption (D'Antonio, 2011; Pappalardo and Mastrolorenzo, 2012). By means of the  
342 thermometric equation of Masotta et al. (2013), we have calculated the crystallization  
343 temperature of the Campanian Ignimbrite assuming a melt-water content of 3 wt.% (see  
344 Pappalardo and Mastrolorenzo, 2012 and references therein). Fig. 5b shows that temperature  
345 predictions widely range from 875 to 1050 °C. However, near-equilibrium data cluster at

346 900±20 °C and, with respect to this value, the error of temperature estimate may be very high  
347 (ETE<sub>max</sub> = 107 °C) for disequilibrium compositions (Fig. 5b). It is worth stressing that Fowler  
348 et al. (2007) have performed calculations based on multicomponent-multiphase equilibria for  
349 the Campanian Ignimbrite. Results revealed a pseudo-invariant temperature of ~883 °C, at  
350 which the fraction of melt remaining in the system decreased from 0.5 to <0.1 (Fowler et al.,  
351 2007). According to the authors, this pseudo-invariant temperature caused abrupt changes in  
352 the composition properties (density, dissolved water content) and physical state (viscosity,  
353 volume fraction fluid) of magma, triggering the eruption. We emphasize that our pre-eruptive  
354 temperature of 900±20 °C is comparable to the onset temperature obtained by Fowler et al.  
355 (2007). This leads to the conclusion that the approach presented in this study is suitable to (i)  
356 identify equilibrium clinopyroxene-melt pairs, (ii) minimize the error on temperature  
357 estimate, and (iii) predict the pre-eruptive temperature of heterogeneous eruptions.

358

#### 359 **4. CONCLUSIONS**

360 The evolution of chemically and thermally zoned magma chambers is frequently  
361 associated to disruption processes leading to the occurrence of different modes of  
362 clinopyroxene and glass in the same eruptive unit. Using equilibrium and disequilibrium  
363 clinopyroxene-melt pairs from isothermal and thermal gradient experiments, we demonstrate  
364 that equilibrium compositions can be identified through the difference between predicted and  
365 measured components in clinopyroxene. This finding has a paramount importance for  
366 retrieving the pre-eruptive temperature of clinopyroxene-bearing heterogeneous eruptions by  
367 reducing the error of temperature estimate caused by the accidental use of disequilibrium  
368 compositions.

369

#### 370 **ACKNOWLEDGEMENTS**



371 A. Cavallo is acknowledged for assistance during electron microprobe analysis. SM was  
372 supported by ERC Starting grant 259256 GLASS project. The research activities of the HP-  
373 HT laboratory of the INGV were supported by the European Observing System Infrastructure  
374 Project (EPOS).

375

## 376 REFERENCES

377 Bachmann, O., Deering, C.D., Ruprecht, J.S., Huber, C., Skopelitis, A., Schnyder, C., 2012.  
378 Evolution of silicic magmas in the Kos-Nisyros volcanic center, Greece: cycles associated  
379 with caldera collapse. *Contributions to Mineralogy and Petrology* 163, 151-166.

380 Blake, S., 1981. Volcanism and the dynamics of open magma chambers. *Nature* 289, 783-  
381 785.

382 Blake, S., Ivey, G.N., 1986. Magma-mixing and the dynamics of withdrawal from stratified  
383 reservoirs. *Journal of Volcanology and Geothermal Research* 27, 153-178.

384 Boden, D.R., 1989. Evidence for step-function zoning of magma and eruptive dynamics,  
385 Toquima caldera complex, Nevada. *Journal of Volcanology and Geothermal Research* 37,  
386 39-57.

387 Cathey, H.E., Nash, B.P., 2004. The Cougar Point Tuff: Implications for Thermochemical  
388 Zonation and Longevity of High-Temperature, Large-Volume Silicic Magmas of the  
389 Miocene Yellowstone Hotspot. *Journal of Petrology* 45, 27-58.

390 Civetta, L., Orsi, G., Pappalardo, L., Fisher, R.V., Heiken, G. and Ort, M., 1997. Geochemical  
391 zoning, mingling, eruptive dynamics and depositional processes; the Campanian  
392 Ignimbrite, Campi Flegrei caldera, Italy. *Journal of Volcanology and Geothermal*  
393 *Research* 75, 183-219.

394 Conticelli, S., Francalanci, L., Manetti, P., Cioni, R., Sbrana, A., 1997. Petrology and  
395 geochemistry of the ultrapotassic rocks from the Sabatini volcanic district, central Italy:

396 the role of evolutionary processes in the genesis of variably enriched alkaline magmas.  
397 *Journal of Volcanology and Geothermal Research* 75, 107–136.

398 D'Antonio, M., 2011. Lithology of the basement underlying the Campi Flegrei caldera:  
399 volcanological and petrological constraints. *Journal of Volcanology and Geothermal*  
400 *Research* 200, 91-98.

401 Deering, C., Cole, J., Vogel, T., 2011. Extraction of crystal-poor rhyolite from a hornblende-  
402 bearing intermediate mush: a case study of the caldera-forming Matahina eruption,  
403 Okataina volcanic complex. *Contributions to Mineralogy and Petrology* 161, 129-151.

404 Devine, J.D., Gardner, J.E., Brack, H.P., Layne, G.D., Rutherford, M.J., 1995. Comparison of  
405 microanalytical methods for estimating H<sub>2</sub>O contents of silicic volcanic glasses. *American*  
406 *Mineralogist* 80, 319–328.

407 Evans, B.W., Bachmann, O., 2012. Implications of equilibrium and disequilibrium among  
408 crystal phases in the Bishop Tuff. *American Mineralogist* 98, 271-274.

409 Fabbriozio, A, Carroll, M., 2008. Experimental studies of the differentiation process and pre-  
410 eruptive conditions in the magmatic system of Phlegreans Fields (Naples, Italy). *Journal*  
411 *of Volcanology and Geothermal Research* 171, 88-102.

412 Fedele, L., Scarpati, C., Lanphere, M., Melluso, L., Morra, V., Perrotta, A., Ricci, G., 2008.  
413 The Breccia Museo formation, Campi Flegrei, southern Italy: geochronology,  
414 chemostratigraphy and relationship with the Campanian Ignimbrite eruption. *Bulletin of*  
415 *Volcanology* 70, 1189-1219.

416 Fedele, L., Zanetti, A., Morra, V., Lustrino, M., Melluso, L., Vannucci, R., 2009.  
417 Clinopyroxene/liquid trace element partitioning in natural trachyte-trachyphonolite  
418 systems: insights from Campi Flegrei (southern Italy). *Contributions to Mineralogy and*  
419 *Petrology* 158, 337-356.

420 Fowler, S.J., Spera, F.J., 2010. A metamodel for crustal magmatism: phase equilibria of giant  
421 ignimbrites. *Journal of Petrology* 51, 1783-1830.

422 Fowler S.J., Spera F.J., Bohron, W.A., Belkin H.E., De Vivo B., 2007. Phase Equilibria  
423 Constraints on the Chemical and Physical Evolution of the Campanian Ignimbrite. *Journal*  
424 *of Petrology* 48, 459-493.

425 Fridrich, C.J., Mahood, G.A., 1987. Compositional layers in the zoned magma chamber of the  
426 Grizzly Peak Tuff. *Geology* 15, 299-303.

427 Fulignati, P., Marianelli, P., Santacroce, R., Sbrana, A., 2004. Probing the Vesuvius magma  
428 chamber-host rock interface through xenoliths. *Geological Magazine* 141, 417-428.

429 Ghiorso, M.S., Sack, R.O., 1995. Chemical Mass-Transfer in Magmatic Processes .4. A  
430 Revised and Internally Consistent Thermodynamic Model for the Interpolation and  
431 Extrapolation of Liquid-Solid Equilibria in Magmatic Systems at Elevated-Temperatures  
432 and Pressures. *Contributions to Mineralogy and Petrology* 119, 197-212.

433 Grove, T.L., Bryan, W.B., 1983. Fractionation of pyroxene-phyric MORB at low pressure: an  
434 experimental study. *Contributions to Mineralogy and Petrology* 84, 293–309.

435 Jeffery, A.J., Gertisser, R., Troll, V.R., Jolis, E.M., Dahren, B., Harris, C., Tindle, A.G.,  
436 Preece, K., O'Driscoll, B., Humaida, H., Chadwick, J.P., 2013. Magma plumbing system  
437 of the 2007-2008 dome-forming eruption of Kelut volcano, East Java, Indonesia.  
438 *Contributions to Mineralogy and Petrology* 166, 275-308.

439 Karner, D.B., Marra, F., Renne, P.R., 2001. The history of the Monti Sabatini and Alban Hills  
440 volcanoes: groundwork for assessing volcanic-tectonic hazards for Rome. *Journal of*  
441 *Volcanology and Geothermal Research* 107, 185-219.

442 Marianelli, P., Sbrana, A., Proto, M., 2006. Magma chamber of the Campi Flegrei  
443 supervolcano at the time of eruption of the Campanian Ignimbrite. *Geology* 34, 937–940.

444 Matthews, S.J., Sparks, R.S.J., Gardeweg, M.C., 1999. The Piedras Grandes–Soncor  
445 Eruptions, Lascar Volcano, Chile; Evolution of a Zoned Magma Chamber in the Central  
446 Andean Upper Crust. *Journal of Petrology* 40, 1891–1919.

447 Masotta, M., Gaeta, M., Gozzi, F., Marra, F., Palladino, D.M., Sottili, G., 2010. H<sub>2</sub>O- and  
448 temperature-zoning in magma chambers: the example of the Tufo Giallo della Via  
449 Tiberina eruptions (Sabatini Volcanic District, central Italy). *Lithos* 118, 119–130.

450 Masotta, M., Freda, C., Gaeta, M., 2012. Origin of crystal-poor, differentiated magmas:  
451 insights from thermal gradient experiments. *Contributions to Mineralogy and Petrology*  
452 163, 49-65.

453 Masotta, M., Mollo, S., Freda, C., Gaeta, M., Moore, G., 2013. Clinopyroxene–liquid  
454 thermometers and barometers specific to alkaline differentiated magmas. *Contributions to*  
455 *Mineralogy and Petrology*, doi: 10.1007/s00410-013-0927-9.

456 Melluso, L., Morra, V., Perrotta, A., Scarpati, C., Adabbo, M., 1995. The eruption of the  
457 Breccia Museo (Campi Flegrei, Italy): fractional crystallization processes in a shallow,  
458 zoned magma chamber and implications for the eruptive dynamics. *Journal of*  
459 *Volcanology and Geothermal Research* 68, 325-339.

460 McGuire, A.V., Dyar, M.D., Ward, K.W., 1989. Neglected Fe<sup>3+</sup>/Fe<sup>2+</sup> ratios: a study of Fe<sup>3+</sup>  
461 content of megacrysts from alkali basalts. *Geology* 17, 687–690.

462 Mollo, S., Del Gaudio, P., Ventura, G., Iezzi, G., Scarlato, P., 2010. Dependence of  
463 clinopyroxene composition on cooling rate in basaltic magmas: Implications for  
464 thermobarometry. *Lithos* 118, 302-312.

465 Mollo, S., Misiti, V., Scarlato, P., Soligo, M., 2012. The role of cooling rate in the origin of  
466 high temperature phases at the chilled margin of magmatic intrusions. *Chemical Geology*  
467 322-323, 28-46.

468 Mollo, S., Lanzafame, G., Masotta, M., Iezzi, G., Ferlito, C., Scarlato, P., 2011. Cooling  
469 history of a dike as revealed by mineral chemistry: A case study from Mt. Etna volcano.  
470 *Chemical Geology* 283, 261–273.

471 Mollo, S., Putirka, K., Misiti, V., Soligo, M., Scarlato, P., 2013. A new test for equilibrium  
472 based on clinopyroxene-melt pairs: Clues on the solidification temperatures of Etnean  
473 alkaline melts at post-eruptive conditions. *Chemical Geology* 352, 92-100.

474 Pabst, S., Worner, G., Civetta, L., Tesoro, R., 2008. Magma chamber evolution prior to the  
475 Campanian Ignimbrite and Neapolitan Yellow Tuff eruptions (Campi Flegrei, Italy).  
476 *Bulletin of Volcanology* 70, 961–976.

477 Pappalardo, L., Mastrolorenzo, G., 2012. Rapid differentiation in a sill-like magma reservoir:  
478 a case study from the Campi Flegrei caldera. *Scientific Reports* 2:712.

479 Pappalardo, L., Ottolini, L., Mastrolorenzo, G., 2008. The Campanian Ignimbrite, Southern  
480 Italy. geochemical zoning, insight on the generation of a super-eruption from catastrophic  
481 differentiation and fast withdrawal. *Contributions to Mineralogy and Petrology* 156, 1–26.

482 Pappalardo, L., Civetta, L., De Vita, S., Di Vito, M.A., Orsi, G., Carandente, A., Fisher, R.V.,  
483 2002. Timing of magma extraction during the Campanian Ignimbrite eruption (Campi  
484 Flegrei caldera). *Journal of Volcanological Geothermal Research* 114, 479-497.

485 Putirka, K., Johnson, M., Kinzler, R., Walker, D., 1996. Thermobarometry of mafic igneous  
486 rocks based on clinopyroxene-liquid equilibria, 0-30 kbar. *Contributions to Mineralogy  
487 and Petrology* 123, 92-108.

488 Putirka, K., 1999. Clinopyroxene + liquid equilibria. *Contributions to Mineralogy and  
489 Petrology* 135, 151-163.

490 Putirka, K., Ryerson, F.J., Mikaelian, H., 2003. New igneous thermobarometers for mafic and  
491 evolved lava compositions, based on clinopyroxene+liquid equilibria. *American  
492 Mineralogist* 88, 1542-1554.

493 Putirka, K.D., 2008. Thermometers and barometers for volcanic systems. In: Putirka, K.D.,  
494 Tepley, F. (Eds.), *Minerals, Inclusions, and Volcanic Processes: Reviews in Mineralogy*  
495 *and Geochemistry*, 69, pp. 61-120.

496 Rolandi, G., Bellucci, F., Heizler, M.T., Belkin, H.E., De Vivo, B., 2003. Tectonic controls on  
497 the genesis of ignimbrites from the Campanian Volcanic Zone, southern Italy. *Mineralogy*  
498 *and Petrology* 79, 3-31.

499 Schuraytz, B.C., Vogel, T.A., Younker, L.W., 1989. Evidence for dynamic withdrawal from a  
500 layered magma body; the Topopah Spring Tuff, southwestern Nevada. *Journal of*  
501 *Geophysical Research* 94, 5925-5942.

502 Signorelli, S., Vaggelli, G., Francalanci, L., Rosi, M., 1999. Origin of magmas feeding the  
503 Plinian phase of the Campanian Ignimbrite eruption, Phlegrean Fields (Italy); constraints  
504 based on matrix glass and glass-inclusion compositions. *Journal of Volcanology and*  
505 *Geothermal Research* 91, 199-220.

506 Sisson, T.W., Grove, T.L., 1993. Experimental investigations of the role of water in  
507 calcalkaline differentiation and subduction zone magmatism. *Contributions to Mineralogy*  
508 *and Petrology* 113, 143–166.

509 Streck, M.J., Grunder, A.L., 1997. Compositional gradients and gaps in high-silica rhyolites  
510 of the Rattlesnake Tuff, Oregon. *Journal of Petrology* 38, 133-163.

511 Wallace, P.J., Anderson, A.T., Jr., Davis, A.M., 1999. Gradients in H<sub>2</sub>O, CO<sub>2</sub>, and exsolved  
512 gas in a large-volume silicic magma system. *Journal of Geophysical Research* 104,  
513 20097–20122.

514 Wark, D.A., Hildreth, W., Spear, F.S., Cherniak, D.J., and Watson, E.B., 2007. Pre-eruption  
515 recharge of the Bishop magma system. *Geology* 35, 235–238.

516 Webster, J.D., Raia, R., Tappen, C., De Vivo, B., 2003. Pre-eruptive geochemistry of the  
517 ignimbrite-forming magmas of the Campanian Volcanic Zone, Southern Italy, determined  
518 from silicate melt inclusions. *Mineralogy and Petrology* 79, 99–125.

519 Zollo, A., Maercklin, N., Vassallo, M., Dello Iacono, D., Virieux, J., Gasparini, P., 2008).  
520 Seismic reflections reveal a massive melt layer feeding Campi Flegrei caldera.  
521 *Geophysical Research Letters* 35, L12306.

522

### 523 **FIGURE CAPTIONS**

524 Figure 1. (a) Sketch drawn of a temperature gradient experiment. The distribution of  
525 clinopyroxene in the capsule suggests the occurrence of crystal settling and melt extraction  
526 processes. The temperature gradient contributes to the formation of chemical gradients in the  
527 melt whose composition changes from tephriphonolite to phonolite. (b) Clinopyroxene-melt  
528 pairs from temperature gradient experiments exhibit strong compositional variations as  
529 revealed by the comparison between the diopside (Di) in clinopyroxene and SiO<sub>2</sub> of the melt .

530

531 Figure 2. (a) Clinopyroxene-melt pairs from isothermal and temperature gradient experiments  
532 have been used as input data for equation (1) and DiHd<sup>Cpx</sup> (diopside + hedenbergite) values  
533 predicted compared with those measured. (b) Isothermal experiments show a  $\Delta\text{DiHd} < 0.02$ .  
534 This threshold defines the equilibrium clinopyroxene-liquid pairs. These pairs show a linear  
535 correlation between the magnesium number of the melt (<sup>melt</sup>Mg#) and that of clinopyroxene  
536 (<sup>cpx</sup>Mg#). The correlation line (<sup>melt</sup>Mg#- <sup>cpx</sup>Mg#) obtained by MELTS is reported for  
537 comparison.

538

539 Figure 3. (a) Both equilibrium and disequilibrium data from our experiments fall within the  
540 equilibrium range of  $0.27 \pm 0.03$  for <sup>cpx-melt</sup>Kd<sub>Fe-Mg</sub> although the  $\Delta\text{DiHd}$  of the majority of these

541 pairs is above the 0.02 equilibrium threshold. (b) The temperature predicted by the  
542 thermometric equation of [Masotta et al. \(2013\)](#) is plotted against the value for <sup>melt</sup>Mg#.  
543 Equilibrium clinopyroxene-melt pairs show errors of temperature estimate (ETE) comparable  
544 to the standard error of estimate of the thermometer (SEE = 18 °C), whereas the error of  
545 temperature estimate of disequilibrium data is on average higher (ETE<sub>max</sub> = 85 °C).

546

547 Figure 4. (a) Clinopyroxene-melt pairs from the Tufo Giallo della Via Tiberina (TGVT)  
548 eruptive sequence are used as input data for equation (1). In the <sup>cpx</sup>Mg# vs. <sup>melt</sup>Mg# diagram,  
549 equilibrium data captured by equation (1) show a linear correlation similar to that obtained  
550 through experimental data reported in Fig. 2b. The correlation line (<sup>melt</sup>Mg#-<sup>cpx</sup>Mg#) obtained  
551 by MELTS is reported for comparison. (b) The temperature predicted by the thermometer of  
552 [Masotta et al. \(2013\)](#) is compared with the difference between predicted and observed  
553 components in clinopyroxene ( $\Delta\text{DiHd}$ ). Equilibrium data predict temperatures that cluster at  
554  $890\pm 25$  °C; conversely, temperatures estimated through disequilibrium data show higher  
555 uncertainties up to a maximum value of ETE<sub>max</sub> = 100 °C.

556

557 Figure 5. (a) The SiO<sub>2</sub> of the melt is compared with diopside (Di) in clinopyroxene from the  
558 Campanian Ignimbrite eruption. Clinopyroxene-melt pairs reported in previous studies show a  
559 scattered compositional distribution. (b) Equilibrium and disequilibrium data have been  
560 resolved through equation (1). Near-equilibrium clinopyroxene-melt pairs ( $\Delta\text{DiHd} \leq 0.02$ )  
561 indicate a pre-eruptive temperature of  $900\pm 20$  °C; in contrast, the use of disequilibrium data  
562 causes an increasing uncertainty showing a maximum value of ETE<sub>max</sub> = 107 °C.

563

564



Figure1  
[Click here to download high resolution image](#)

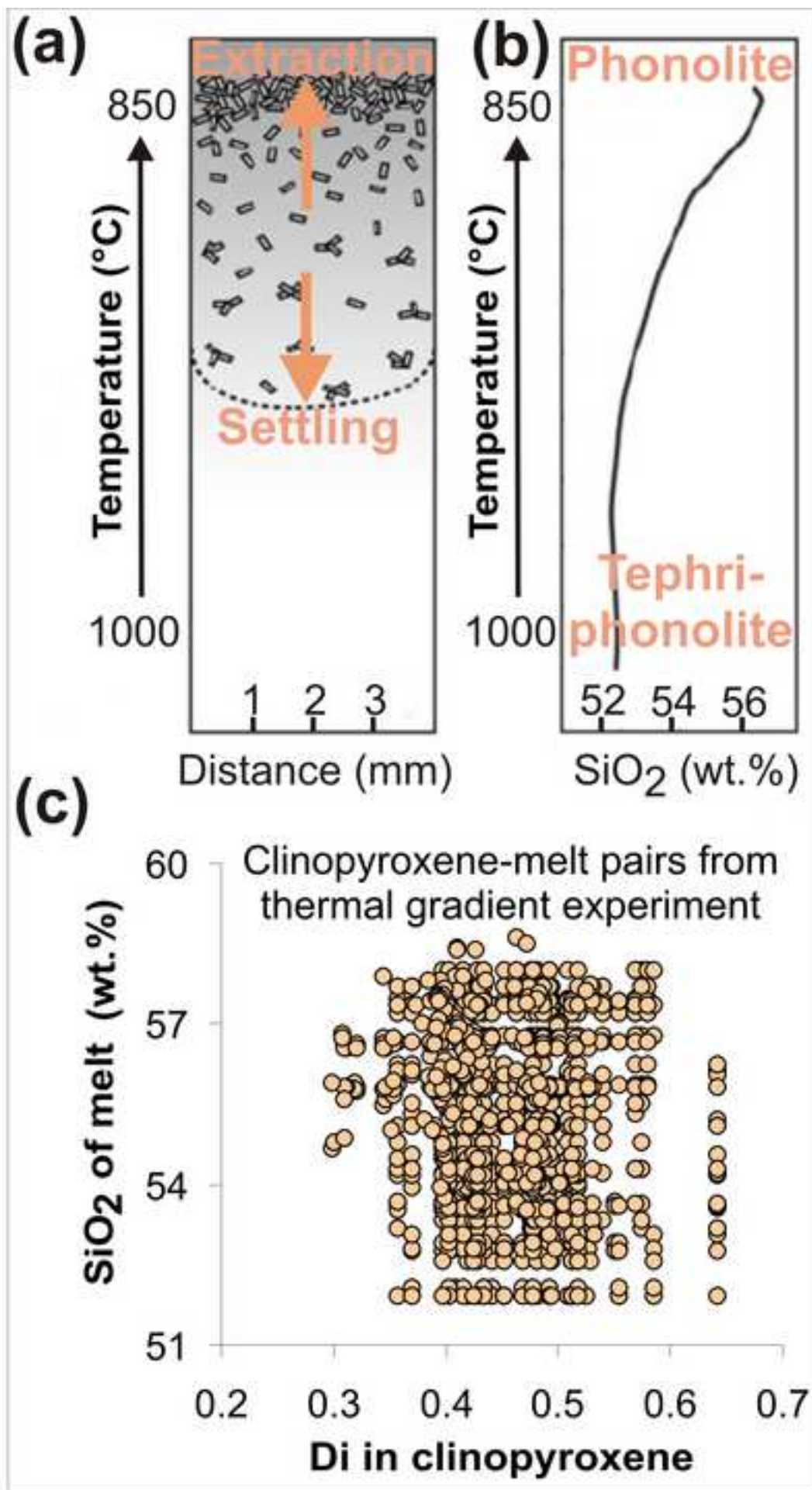


Figure2

[Click here to download high resolution image](#)

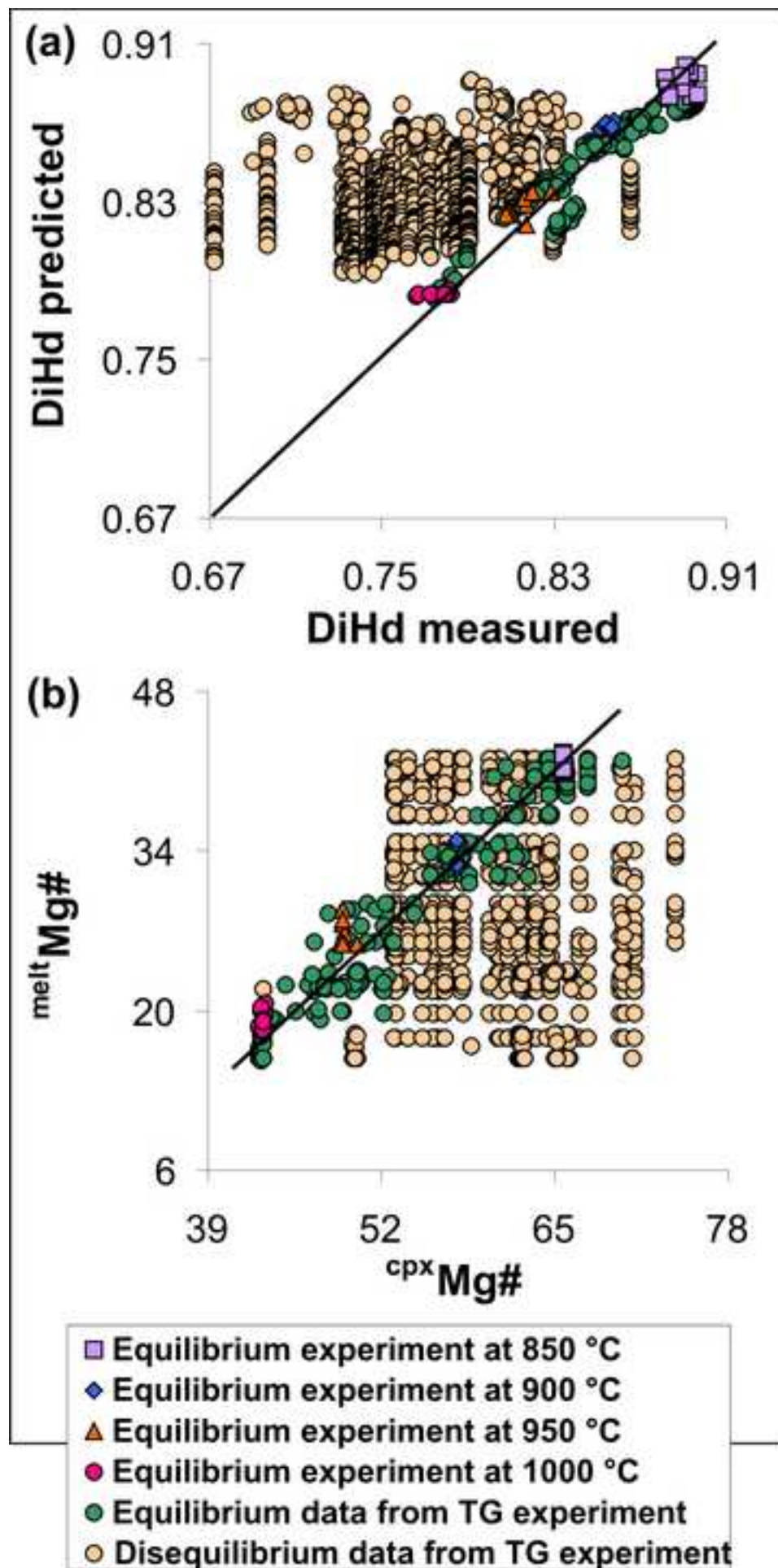


Figure3  
[Click here to download high resolution image](#)

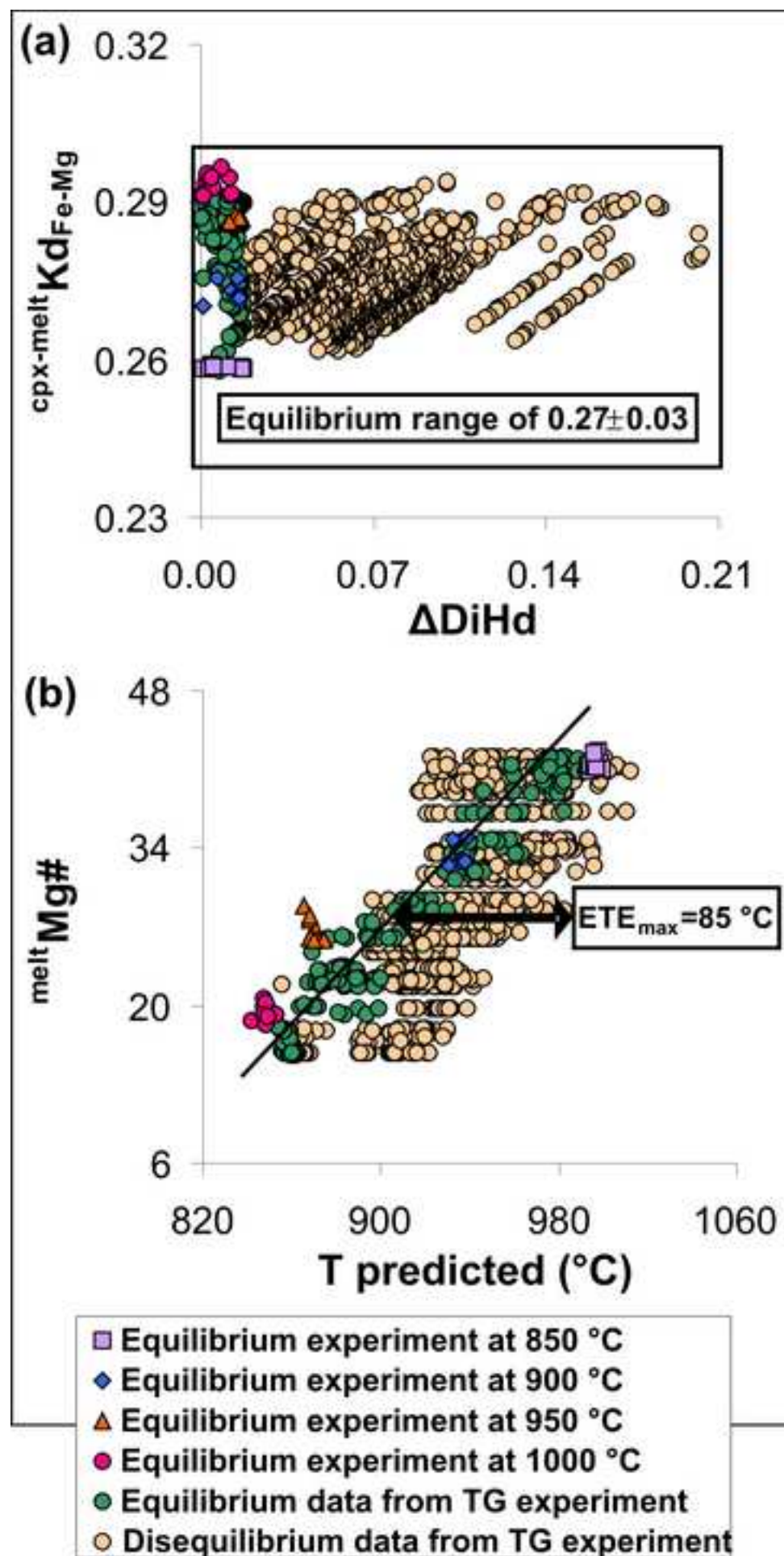


Figure4  
[Click here to download high resolution image](#)

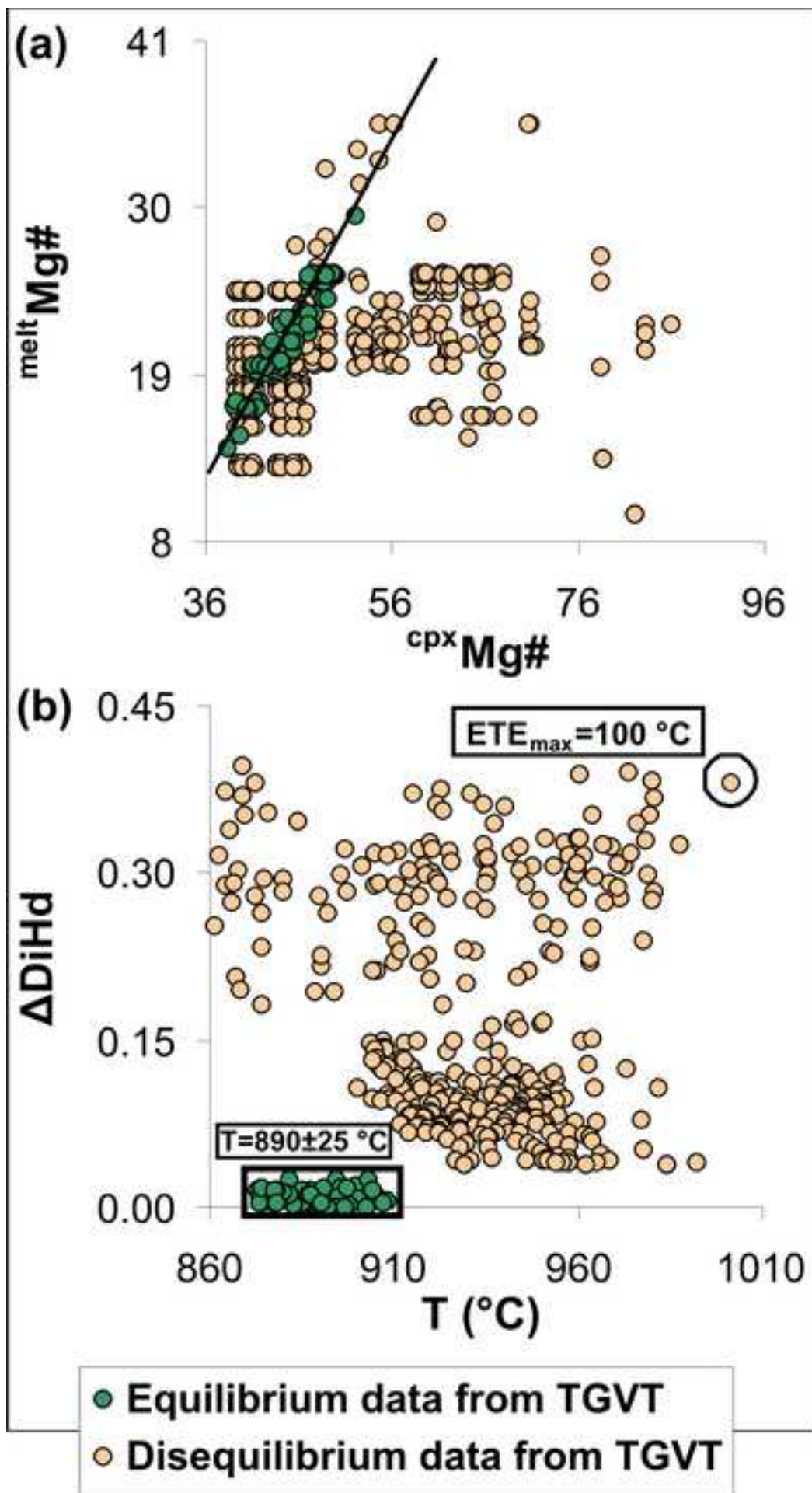
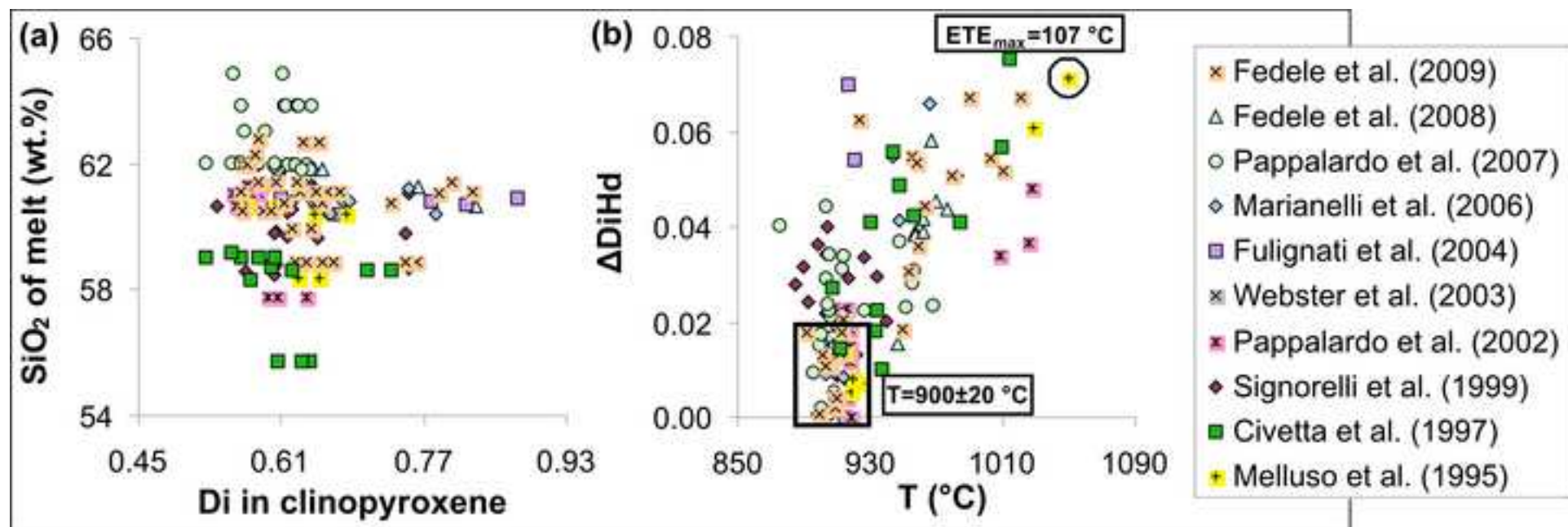


Figure5

[Click here to download high resolution image](#)



**Background dataset for online publication only**

**[Click here to download Background dataset for online publication only: Spreadsheet based on RIMG models\\_Mollo and Masotta](#)**